Computers in Biology and Medicine 42 (2012) 590–597

Contents lists available at SciVerse ScienceDirect

Computers in Biology and Medicine

journal homepage: www.elsevier.com/locate/cbm

Comparison of different EEG features in estimation of hypnosis susceptibility level

Golnaz Baghdadi, Ali Motie Nasrabadi *

Biomedical Engineering Department, Shahed University, Across Emam Khomeini Holy Shrine, Persian Gulf Highway, Tehran, Iran

ARTICLE INFO

Article history:
Received 1 February 2011
Accepted 12 February 2012

Keywords:
Hypnosis
Hypnotizability
EEG signals feature
Classification

ABSTRACT

Hypnosis has long been known to be associated with heightened control over physical processes and researchers put it under consideration because of its usage as a therapeutic tool in many medical and psychological problems. Determination of hypnosis susceptibility level is important before prescribing any hypnotic treatment. In this study different features are introduced to classify hypnotizability levels. These features were extracted from electroencephalogram (EEG) signals which were recorded from 32 subjects during hypnosis suggestion. Based on the obtained result, a method was suggested to estimate the hypnosis susceptibility level from hypnosis EEG signals instead of using traditional clinical subjective tests.

1. Introduction

Hypnosis is seen as a state of focused attention, concentration and inner absorption with a relative suspension of peripheral awareness, which has been used in treatment of different diseases [1]. Most hypnotic inductions include suggestions for relaxation. Individuals differ in hypnotizability. Hypnotizability is rated after the subjects' ability to attain a deep hypnotic stage [2]. In order to clarify the basic physiological conditions for potentially successful hypnosis treatment, determination of subject hypnotizability level is important after hypnosis induction. Hypnosis treatment reportedly is much more successful in high- than low-hypnotizable patients [2]. Currently, hypnotizability level is determined by the use of different standard clinical subjective tests, which measure how well a subject conforms to the behavior of different hypnotizable groups [3–9]. But these clinical tests lead to some problems in determination of hypnosis susceptibility levels (such as (1) performing some of the required tasks in these methods inhibits deepening of hypnosis, (2) being subjective that is the result of these common tests depends on the subject's responses, (3) the time duration of performing these clinical tests is too long, about 45 min, which makes the subject tired and reduces the depth of hypnosis trance and (4) the potential biases and inaccuracies of subjective reports and observations of the hypnotizer). Therefore, in order to avoid the drawbacks of these subjective clinical tests, investigators have tried to find some methods to identify hypnosis susceptibility level of a hypnotized subject based on electroencephalogram (EEG) characteristics.

As the various EEG frequency bands are known to represent different brain functions [10], there have been many studies on the relationship between brainwave activity and hypnosis susceptibility level, for a review, see [11]. These studies reported various differences between high- and low-hypnotizable subjects, but there is no complete agreement between their findings, however a considerable number of these approaches showed a strong relationship between theta and hypnotizability [2,12]. Inconsistencies in the results of these studies might be because of the nature of the suggestions (e.g., for pain relief, relaxation, hallucinations, etc.) that have been used to induce hypnosis.

Recently techniques from nonlinear dynamic view such as fractal dimensionality measures [13], long-range temporal correlations [14] and weighted regional frequency [15] have been introduced for analyzing hypnosis EEG and their relation with hypnotizability. The results of these studies show significant relation between the extracted features from EEG signals and hypnotizability.

As the data (EEG signals of hypnotized subjects) and the hypnosis induction methods are different in the mentioned studies, comparing the results and presenting the best feature that can make the most significant difference between hypnotizable groups is not possible. In the current research in order to find the best feature that can significantly separate different hypnotizable groups, we have implemented the previously reported features. In addition to these features, two new features, empirical mode decomposition (EMD) entropy and phase coherence were also examined in this study. Both features are new in the context of hypnosis EEG analysis; however these were used in different fields [16,17].

The previous studies investigated the relation between the features and hypnotizability statistically and their main goal was to find if the hypnotizability level can affect the selected feature or not. But the goal of the current study is to build a system which

* Corresponding author. Tel.: +98 2151213159.
E-mail addresses: golnaz_baghdadi@yahoo.com (G. Baghdadi), nasrabadi@shahed.ac.ir (A.M. Nasrabadi).

0010-4825/$ - see front matter © 2012 Elsevier Ltd. All rights reserved.
doi:10.1016/j.compbiomed.2012.02.003

can recognize the EEG patterns that significantly belong to different hypnotizability levels.

The stages of this research will be explained more in the following parts. The characteristics of the data and the decomposition algorithm are introduced in Section 2. Section 3 includes explanation of different feature extraction methods. The introduction of the statistical analysis and the classification method is in Section 4 and the results of investigating the ability of different EEG features are brought in Sections 5 and 6.

2. Materials and methods

2.1. Data and subjects

In this research we have used the data that Nasrabadi, (2002) recorded them in his research [18] on "quantitative and qualitative evaluation of consciousness variation and depth of hypnosis". These data contain EEG data of 32 males, right-handed individuals were recorded from 19 electrodes placed according to the standard 10–20 system at a sampling rate of 256 Hz. Hypnosis induction was performed by playing an audiotape based on the Waterloo–Stanford criterion [3,8]. Therefore, the method and the duration of hypnosis induction were the same for all subjects. The first 15 min of this tape was related to the hypnosis induction and the remaining 30 min was related to 12-item Waterloo–Stanford group scale (WSGS) of hypnosis susceptibility measuring. In order to evaluating and comparing the new method's results with a subjective method, a score of hypnotizability was determined for each subject based on WSGS. In the WSGS subjective method, the subjects fill the form after their trance, and then based on the subject's answer in the filled form a hypnosis susceptibility score (a number between 12 and 60 according to the WSGS guidelines) is determined for each subject. Based on these scores, the subjects were divided into the low ($12 < \text{WSGS scores} < 22$), medium ($23 < \text{WSGS scores} < 41$) and high ($42 < \text{WSGS scores} < 60$) hypnotizable groups. In our dataset, 4 subjects were categorized as low, 18 subjects as medium and 10 subjects as high hypnotizable.

2.2. Brainwave decomposition

Among all available time–frequency analysis methods, the wavelet transform may be the best one [19]. However, the wavelet transform still has some inevitable defects, including the interference terms, border distortion and energy leakage, all of which will generate a lot of small undesired spikes all over the frequency scales and make the results confusing and difficult to be interpreted. Moreover wavelet analysis is still convolutional and the mother wavelet is problem dependent. Another important limitation of the wavelet analysis is its non-adaptive nature. Once the basic wavelet is selected, one will have to use it to analyze all the data. This leads to an assumption on the characteristic of the analyzed signal. As a consequence, only signals feature that correlate well with the shape of the wavelet function have a chance to lead to coefficients of high value. All other features will be masked or completely ignored [19].

In this study, a new decomposing algorithm was used for analyzing the EEG data. This method is called Haung–Hilbert transform that is the combination of empirical mode decomposition (EMD) algorithm [20] and Hilbert transform [21]. Unlike other approaches such as Fourier and Wavelet transforms, this algorithm does not make any assumptions about the signal and estimates the spectral information of the signal at each time instant by decomposing the signal in time domain. The Haung–Hilbert method is an appropriate method for analyzing non-linear and non-stationary signals that is the case for EEG signal [22].

EMD method is an adaptive data driven decomposition procedure, decomposes a time series into a finite and often small number of intrinsic mode functions (IMFs), each of which must satisfy the following definition:

(1) Number of extrema = number of zero-crossings ± 1.
(2) At any point, the mean value of the upper and lower envelope is zero.

The IMFs, $x_i(t)$, of a signal $y(t)$, is found as follow [23]:

(1) Compute the mean of upper and lower envelopes of signal, $m(t)$.
(2) Subtract to the signal to obtain $z_i(t) = y(t) - m(t)$.
(3) Check if $z_i(t)$ is an IMF, then $z_i(t)$ is the first IMF of y(t). If it is not an IMF, $z_i(t)$ is treated as the original signal and (1)–(3) are repeated;
(4) Separating $z_i(t)$ from $y(t)$, we get $y_i(t) = y(t) - z_i(t)$. $y_i(t)$ is treated as the original data, and by repeating the above processes, the second IMF of $y(t)$ could be obtained.

The second step is applying Hilbert transform to each IMF, in order to compute the instantaneous frequency and amplitude at each time. $X(t)$ in the following equation is the Hilbert transform of $Y(t)$.

$$X(t) = Hilbert\ \ Tranform\{Y(t)\} = \frac{1}{\pi}\int_{-\infty}^{\infty}\frac{Y(t)}{t-t'}dt' \tag{1}$$

Using Eq. (1), instantaneous frequency, $f(t)$, and instantaneous amplitude, $a(t)$, are defined as [23]:

$$a(t) = \sqrt{Y^2(t) + X^2(t)} \begin{cases} f(t) = \frac{d\theta(t)}{2\pi dt} \\ \theta(t) = \arctan\left[\frac{X(T)}{Y(T)}\right] \end{cases} \tag{2}$$

Computing the energy of the considered frequency band (Delta, Theta, Alpha, Beta and Gamma) is done by computing the energy of the sum of the IMFs that belong, at each sample, to the considered frequency band [24]. The relative energy for each frequency band was computed by dividing the integrated value by the total power in the whole frequency bands.

3. The features

3.1. Brainwave energy based on EMD method

Using the combination of EMD algorithm and Hilbert transform, instantaneous amplitude and frequency of the signals were extracted. Squaring the instantaneous amplitudes of each frequency band was used to calculate brainwave instantaneous energy. In this project, three types of energy were calculated in various frequency bands, maximum energy, average energy and relative energy. Maximum energy is the greatest energy value in a considered time window. Calculating the mean energy along a time window gives the average energy and relative energy for each frequency band was computed by dividing the integrated value by the total power in the whole extracted bands.

3.2. Fractal dimension

Fractal dimension (FD) analysis provides a computational tool to track complexity variations of nonlinear signal. Applying Higuchi's [25] and Petrosian's [26] algorithm, we have calculated FD values.

3.2.1. Higuchi's algorithm

In calculating Higuchi's dimension, briefly, if we consider EEG signal as a time sequence $x(1), x(2) \ldots, x(n)$, we may construct k

new self-similar (fractal) time series $x(k,m)$ as:

$$x(k,m) = \{x(m), x(m+k), \ldots, x(m+\mathrm{int}[(N-m)/k]k)\} \tag{3}$$

For $m=1,2,\ldots,k$ and $int[.]$ as an integer function. We computed the length $L(m,k)$ for each of the k time series or curves $x(k,m)$:

$$L(m,k) = \frac{\sum_{i=1,\mathrm{int}[(n-m)/k]} |x(m+ik)-x(m+(i-1)k)|(n-1)}{\mathrm{int}[(n-m)/k]k} \tag{4}$$

$L(m,k)$ was averaged for all m forming the mean value of the curve length $L(k)$, for each k. Thus, we obtained an array of mean values $L(k)$, and then from the plot of $log(L(k))$ versus $log(1/k)$, we estimated the fractal dimension (FD) as the slope of least squares linear best fit [25]:

$$FD = \log(L(k))/\log(1/k) \tag{5}$$

3.2.2. Petrosian's algorithm

This algorithm presented a quick estimate of the fractal dimension that is computed as [27]:

$$D = \frac{\log_{10}^{n}}{\log_{10} n + \log_{10}(n/(n+0.4\times N))} \tag{6}$$

where n is the length of the sequence and N is the number of sign changes in the derivative of the signal and as the signal is digital, the derivative is obtained by subtracting consecutive series.

3.3. Scaling exponent

Scaling exponent is important in the characterization of long-range temporal correlations in finite-length sequences. Temporal coherence describes the correlation or predictable relationship between signals observed at different moments in time [13]. Self-similarity parameter or scaling exponent, which is calculated by detrended fluctuation analysis (DFA) as follow:

(1) Alter the given signal x_i into integrated series, $\langle x_i \rangle$ represents the average value of x_i:

$$X_t = \sum_{i=1}^{t} (x_i - \langle x_i \rangle) \tag{7}$$

(2) Calculate the root-mean-square deviation from the local trend (fluctuation), X_n, over every window with size L:

$$F(L) = \left[\frac{1}{L}\sum_{i=1}^{L}(X_i - X_n)^2\right]^{1/2} \tag{8}$$

(3) This detrending is repeated over the whole signal at a range of different window sizes L, and a graph of log (L) against log ($F(L)$) is constructed.

(4) The scaling exponent α is calculated as the slope of a straight line fit to this log–log graph using least squares. By this method, scaling exponent can have different values [14]:
- $\alpha < 1/2$: anti-correlated
- $\alpha \approx 1/2$: uncorrelated
- $\alpha > 1/2$: correlated
- $\alpha \approx 1$: 1/f-noise
- $\alpha > 1$: non-stationary, random walk like,
- $\alpha \approx 3/2$: Brownian motion

3.4. EMD entropy

If n IMFs and a residue r_n are obtained using the EMD method to decompose the hypnosis EEG signal $x(t)$ where the energy of the n IMFs is $E_1, E_2, \ldots, E_n$, respectively; the sum of the energy of the n IMFs is equal to the total energy of the original signal. As the IMFs $c_1(t), c_2(t), \ldots, c_n(t)$ include different frequency components, $E=\{E_1, E_2, \ldots, E_n\}$, forms an energy distribution in the frequency domain of EEG signals, and then the corresponding EMD energy entropy is designated as [17]:

$$H_{EN} = -\sum_{i=1}^{n} p_i \log p_i \tag{9}$$

where $p_i = E_i/E$ is the percent of the energy of $c_i(t)$ in the whole signal energy $E = \sum_{i=1}^{n} E_i$.

3.5. Phase coherence

Phase synchronization has been observed for weakly coupled chaotic self-sustained signals. This theory has been generalized to stochastic signals. To detect phase synchronization between two signals, phase and amplitude of the signals have to be calculated [16]. In this study, using Eq. (2), the phase and amplitude information has been extracted.

Mean phase coherence, $R_{1,1}$, is an index of phase synchronization which is measured as follows:

$$R_{1,1}^2 = \langle \cos \Psi(t) \rangle^2 + \langle \sin \Psi(t) \rangle^2,$$
$$\Psi(t) = (\Phi^{(1)}(t) - \Phi^{(2)}(t)) \bmod 2\pi \tag{10}$$

where $\Phi^i(t)$ denotes the phase of time series i. Taking values of $R_{1,1}$ close to zero if there is no phase synchronization between two signals [27,28].

3.6. Weighted frequency

Eq. (2) gives the frequencies and their amplitudes that make a signal in each time. Investigating the time–frequency–amplitude spectrum of a signal shows that a number of frequencies have larger amplitude and this subject offers that these frequencies are more dominant in each time; but a simple average of all obtained frequencies in each time does not consider the larger effect of the dominant frequencies. This problem can be solved by considering a larger weight for the dominant frequencies in calculating the average frequency in each time. In this study the weight of each instantaneous frequency, $If_j(t)$, is the instantaneous amplitude of this frequency, $a_j(t)$, divided by the summation of all instantaneous frequency's amplitudes, see Eq. (11). Therefore, the weight of the instantaneous frequencies that have the larger amplitude is greater than those that have lower amplitude others.

$$WIF(t) = \sum_{j=1}^{n} a_j(t) If_j(t) / \sum_{j=1}^{n} a_j(t) \tag{11}$$

where n is the number of the IMFs of a signal which is recorded from one of the brain channels. $If_j(t)$ and $a_j(t)$ is the series of the estimated instantaneous frequency and amplitude for each IMF [29,30]. $WIF(t)$ is a series of weighted instantaneous frequency. In this study we used the average of $WIF(t)$ in time windows of the hypnosis EEG, so we have used weighted frequency instead of instantaneous frequency:

$$WF = \sum_{t=t'}^{t'+T} WIF(t) \tag{12}$$

In this equation, WF is the average of WIFs in a time window that its duration is T [15].

4. Statistical analysis and classifier

4.1. ANOVA and MANOVA

Before designing and using any classifier, it was tested that if the extracted features can make significant difference between three hypnotizable groups or not. This investigation was performed using some statistical analyses such as analysis of variance (ANOVA) [31] and multivariate analysis of variance (MANOVA) [32,33]. The normality of the data was investigated before performing the analyses. The Lilliefors test [34] was employed for goodness of fit the data to a normal distribution. Based on the result of this test, the hypothesis that the data has a normal distribution was accepted at significance level 0.05. ANOVA was used when one feature was employed for making difference between three hypnotizable groups and MANOVA was used in condition that the ability of simultaneously usage of different features was investigated. The MANOVA can also give a linear combination of the different features that makes the largest separation between groups. The calculation of the coefficients of this linear combination was done by maximizing the F ratio:

$$F = \frac{\vec{W}^T \Sigma_b \vec{W}}{\vec{W}^T \Sigma \vec{W}} \tag{13}$$

This ratio represents the between groups variability, Σ_b, with respect to within groups variability, Σ. This means that when $\vec{W}$ is an eigenvector of $\Sigma^{-1}\Sigma_b$, the separation will be equal to the corresponding eigenvalue. Therefore, the coefficients of the linear combination maximize the ratio of between-groups to within-group variance.

4.2. K-Nearest neighborhood algorithm

The K-Nearest Neighbors (K-NN) classification is one of the most fundamental and simplest classification methods. K-NN is a type of instance-based learning which does not need to calculate any parameter for making a classifier, in that, like the neural network based classifier, we have not to estimate the classifiers' parameters, for example, the weight of the neurons. In this method, the proximity of neighboring input (x) observations in the training data set and their corresponding output values (y) are used to predict (score) the output values of cases in the validation data set. An object is classified by a majority vote of its neighbors, with the object being assigned to the class most common amongst its K nearest neighbors. K is a positive integer that in the current study we have considered the outcome of KNN based on 3-nearest neighbor (The value of $K(=3)$ was selected based on trial and error method). One of the most common and popular choices to measure the distance in this algorithm is known as Euclidean (Eq. (14)) [35,36], therefore in this case we have used the Euclidean distance as a metric for measuring the adjacency of neighboring input.

$$d_j(x_i,x_j) = \sqrt{\sum_{k=1}^{p} (x_{ip} - x_{jp})^2} \tag{14}$$

where x_i is an input sample with p features ($x_{i1}, x_{i2},\ldots, x_{ip}$), x_j is a sample in the training data set with p features ($x_{j1}, x_{j2},\ldots, x_{jp}$) and $d_j(x_i, x_j)$ is the Euclidean distance between sample x_i and x_j ($j=1,2,\ldots,n$) which n is the total number of samples in the training data set [36].

4.3. Leave-one-out (LOO) cross validation

For evaluating the performance of the KNN based classifier, we have used leave-one-out (LOO) cross validation method. When using the leave-one-out method, the learning algorithm is trained multiple times using all but one of the training set data points. then the removed data point is tested and the error is calculated. This procedure is repeated R times, where R is the number of training set points. Then the mean error is calculated over all R data points. Leave-one-out cross validation is useful, because it use all of the data in test and training stage. Therefore, its result is essentially the same as using all the data points in training stage. This method is so appropriate when the size of the data set is small.

5. Result

Based on the introduced algorithms, the following features were extracted from the subjects' hypnosis EEG data which the investigating result of their performance makes significant difference between three hypnotizable groups will be reported in this part:

- Maximum, average and relative energy of all frequency bands (delta, theta, alpha, beta and gamma) in 19 EEG channels.
- Fractal dimension in 19 EEG channels.
- Scaling exponent in all frequency bands (delta, theta, alpha, beta and gamma) in 19 EEG channels.
- EMD entropy in 19 EEG channels.
- Mean phase coherence in all frequency bands (delta, theta, alpha, beta and gamma) in 19 EEG channels.
- Weighted frequency in 19 EEG channels.

Using statistical tests, between the introduced features and their linear combinations, those who showed that could not make significant difference between three hypnotizable groups, were omitted. Therefore based on the result of the statistical test, best features (the features with small p-values, $p<0.01$) were selected (Table 1).

Table 1
Results of investigating the ability of the selected features for making significant difference between three hypnotizable groups, using statistical tests and a KNN classifier.

	Feature[a]	p-value[b]	Classification error (%)[c]
1	The linear combination of the first 14 IMFs Petrosian's dimension of the signal in channel T6	$3.62e-007$	21.88
2	The linear combination of the first 14 IMFs Higuchi's dimension of the signal in channel T6	$3.78e-007$	6.25
3	The linear combination of the scaling exponent in Theta band in channel C4, Petrosian's dimension and Higuchi's dimension in channel T6	$2.40e-010$	0
4	The linear combination of the EMD entropy in channels Fp2 & F8, Petrosian's dimension and Higuchi's dimension in channel T6	$1.58e-012$	12.5
5	The linear combination of the phase coherence between channels Fp2 & Fz in Delta band, scaling exponent in Theta band in channel C4, Petrosian's dimension and Higuchi's dimension in channel T6	$1.4e-010$	3.13
6	The linear combination of the weighted regional frequency in channels Fp2 & F8, Petrosian's dimension and Higuchi's dimension in channel T6	$9.64e-011$	6.25

[a] The features which their ability to make significant difference between three hypnotizable groups was rejected by the statistical tests, were not shown in this table.
[b] Considered null hypothesis in the statistical tests: there is no significant difference between groups.
[c] The errors were obtained by considering of test data after cross validation with LOO method.

Table 2
Best selected features for classification of low, medium and high hypnotizable groups.

	Feature	Classification error (%)	Priority
1	The linear combination of the first 14 IMFs Higuchi's dimension of the signal in channel T6	6.25	When the reduction of recording electrodes is considered
2	The linear combination of the scaling exponent in Theta band in channel C4, Petrosian's dimension and Higuchi's dimension in channel T6	0	When the reduction of classification error is more important

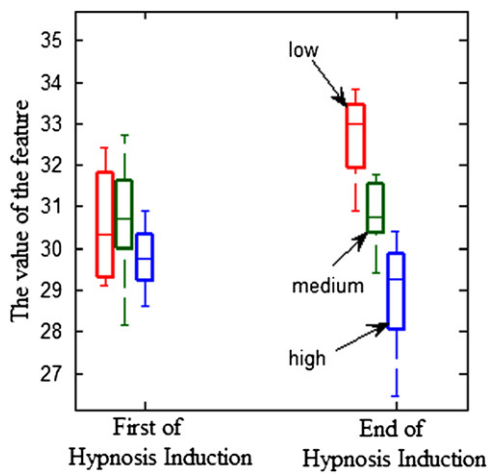

Fig. 1. Distribution of the feature based on the Higuchi's dimension of the signal's IMFs in channel T6 at the beginning and end of hypnosis induction in three hypnotizable groups.

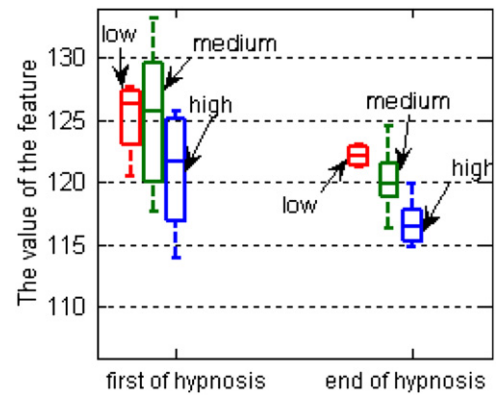

Fig. 2. Distribution of the feature based on the linear combination of the scaling exponent in Theta band in channel C4, Petrosian's dimension and Higuchi's dimension in channel T6 at the beginning and end of hypnosis induction in three hypnotizable groups.

In the other word we used statistical analysis to minimize the features' dimension by omitting the features in different frequency bands or EEG channels that have no role in classifying the hypnotizable groups (in the channels or frequency bands which the feature's p-value was greater than 0.01). In this way in addition to removing non-important features, the importance of different frequency bands and the EEG channels were evaluated and according to the results it seems that considering a special feature, some frequency bands or some EEG channels are more important than others (the first column of Table 1). In order to find an appropriate feature to successful estimation of hypnosis susceptibility level, the selected features were examined again using a KNN classifier ($K=3$). The result was summarized in Table 1.

According to the results in the Table 1, these features which were selected based on statistical analysis ($p<0.01$) and were also evaluated by a KNN based classifier are suitable for classification of three hypnotizable groups, low, medium and high. However, it seems that some of them are more appropriate. For instance, the feature based on Higuchi's dimension (row 2 in Table 1), needs to be calculated just from one channel (T6), while the other introduced features should be calculated from more than one channel. Therefore, whenever the reduction of the recording electrodes is important, using the feature based on the Higuchi's dimension of the signal's IMFs is the best choice that estimates the hypnotizability level by the error of 6.25%. But if increasing the number of the recording electrodes makes no problem and the main goal is reducing classification error, the best feature is the linear combination of (1) the scaling exponent in theta band in channel C4, (2) Petrosian's dimension and the (3) Higuchi's dimension of the signal's IMFs in channel T6 that can classify three hypnosis susceptibly groups with no error.

Therefore we can fulfill our feature selection procedure and say that the study of various extracted features from 19 EEG channels in delta, theta, alpha, beta and gamma frequency bands showed the features which were reported in Table 2 are the best among all of the introduced features for classification of low, medium and high hypnotizable subjects.

Figs. 1 and 2 show, respectively, the distribution of the first feature (the feature based on the Higuchi's dimension of the signal's IMFs in channel T6) and second feature (The linear combination of the scaling exponent in Theta band in channel C4, Petrosian's dimension and Higuchi's dimension in channel T6) at the beginning and end of hypnosis induction in three hypnotizable groups.

According to these figures it was seen that based on the selected features, three hypnotizable groups are separate from each other significantly at the end of hypnosis induction. The results are evaluated and discussed more detailed in the next part.

6. Discussion

According to the results, two features were introduced for classification of three hypnotizable groups (Table 2). Fig. 1 shows that the distributions of the first feature in three hypnotizable groups overlap each other at the beginning of hypnosis induction but the result shows that at the end of hypnosis induction the distribution of this feature is significantly different in three hypnotizable groups. Therefore it can be claimed that based on the selected feature, hypnosis induction has not the same effect on three hypnoyizable groups. In other words Fig. 1 shows that at the end of hypnosis induction high hypnotizable subjects have lower value of the selected feature than the mediums and the mediums have lower value of the selected feature than low hypnotizable group. Therefore, at the end of hypnosis induction between the two subjects, the person who has lower value of the selected feature is more hypnotizable than the other and vice versa. Based on the results and Fig. 2 the same result exists for the second feature.

As it was mentioned in the introduction part traditional clinical subjective methods have different problems in determining a

subject's hypnotizability level. One of these problems is that these methods are subjective and their results depend on the subject's answer and reaction to the clinician's question. Therefore inaccuracies of subjective answers make the results unreliable, and in order to solve this problem the hypnotizer has to ask a question in different way to make sure that the subject's answer is really true or not. The procedure of completing these questions and answers take about 30 min which may be boring for the subject (and also the hypnotizer) and also may the subject be out from the hypnosis, so the EEG based method that was introduced in this research could be a suitable replacement for these traditional subjective methods. The procedure of the determining a subject's hypnotizability level based on the EEG dynamics changes is as follows:

1- Before starting the hypnosis suggestion the clinician connect the EEG electrodes in its appropriate place (T6, if the hypnotizer wants to use the first feature in Table 2 for detecting the subject's hypnosis susceptibility level or both T6 and C4, if the hypnotizer wants to use the second feature in Table 2).
2- Start the hypnosis induction procedure (during the hypnosis induction, the EEG signals of the subject will be recorded).
3- At the end of hypnosis induction, hypnotizer selects the command of characterizing the hypnotizability level from the graphical menu of the software which has been designed for calculating the EEG based features.
4- The software will calculate the selected feature based on the algorithms which were discussed in the previous parts. As it was seen in Figs. 1 and 2 the value range of the features are significantly different in three hypnotizable groups. In the software, the calculated value of the selected feature will be given to the predesigned classifier (KNN) and classifier will determine the subject's hypnotizability level as its output. Calculating the introduced features and division making by the classifier, take less than 2 min (using a pentium4 with 3.2 GHz CPU).

Therefore this EEG based method against traditional subjective method does not need the subject's answer or reaction and does not take a lot of time and just after hypnosis suggestion (less than 2 min) the hypnotizer can say that the subject is a low, medium or high hypnotizable and can start the hypnotherapy if he recognizes that the subject is in an appropriate level of hypnotizability. Fig. 3 shows the block diagram of this procedure.

This figure demonstrates the system which has been proposed, designed and evaluated in this study in order to extract special metrics from the subject's EEG signals (one of the two selected feature in Table 2) and to classify individuals' hypnozability level objectively. Besides the designing of this system which was the aim of this research, the results were also evaluated more from the physiological point of view:

1- According to the results in Table 1 it was seen that the electrode T6 is strongly involved in the classification of hypnosis susceptibility level. This electrode is located in the right side of the temporal lobe. In the study of Ross and Persinger in 1987, it was also reported that temporal lobe activities and hypnotic susceptibility may share a common factor [37]. The temporal lobe is involved in auditory perception and is home to the primary auditory cortex. It is also important in processing semantics in both speech and vision. The temporal lobe contains the hippocampus and plays a key role in the formation of long-term memory [38]. As it was mentioned before hypnosis induction was performed by playing an audiotape based on the Waterloo–Stanford criterion, therefore the subject's auditory sense was more involved in this research and it may be one of the reasons which has exited the temporal lobe in the current study. Kihlstrom et al. (1980) in their study claimed that hypnotic susceptibility is related to the semantic memory [39] and as the temporal lobe has important role in the processing of semantics, it can be concluded that temporal lobe activity relates to the hipnotizablity level. To answer this question that why the right side of the temporal lobe (T6) is involved in the hypnosis, there is evidence in a study which was done by Bick in 1989. In this study, it was claimed that hypnosis switches the brain electrical activities from the left to the right hemisphere in right-handed persons.
2- According to the selected features in Table 2, it seems that theta band activity is related to the hypnotizability level more than the other frequency bands. There are different studies which report that the most solid relationship between EEG activity, hypnosis, and hypnotizability exists in the EEG theta frequency range [40–43]. Theta band is Associated with inhibition of elicited responses (has been found to spike in situations where a person is actively trying to repress a response or action [44]). There is a body of evidence that frontal functions become inhibited during hypnotic induction, for review see ref. [45]. Therefore this repression may be the reason of theta band being raised.
3- The other point which was observed from the results is that among all the examined features, the features which relate to the nonlinear dynamics of a signal (fractal dimensions and scaling exponent that is measured by DFA method) showed the best performance. Traditional techniques decompose the component frequencies in the EEG and thus reflect a limited

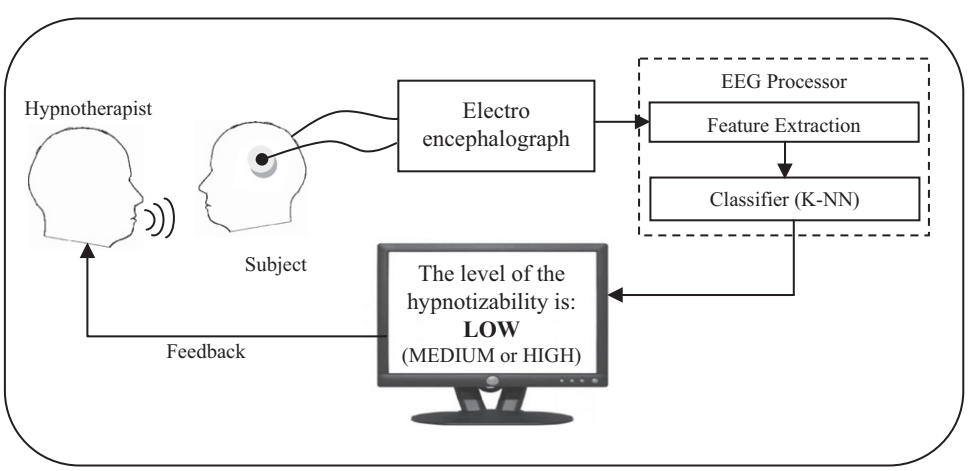

Fig. 3. Block diagram of the proposed system to estimate the subject's hypnotizability level based on EEG recording at the end of hypnosis induction.

amount of information (one dimensional). Recent techniques from nonlinear dynamic view, popularly known as "chaos," (such as fractal dimensions) suggest that a time series may be analyzed to reflect all other variables participating in the dynamics of the system. This approach can give important insight into the interpretation of EEG [13]. It suggests that the complex activity generated by the brain in hypnosis may not be random but indeed contain information concerning the underlying nonlinear process of the brain. According to Fig. 1 it seems that the value range of the fractal dimension is significantly different in three hypnotizable groups. As the fractal dimension is an index of existing correlation (self similarities) in the signal, it can be suggested that hypnotazability level has significant effect on the EEG dynamics and can increase or decrease the signal's temporal correlations. The previous studies showed that the amplitude of EEG oscillations in the human brain possesses long-range temporal correlations, see [13] for a review. Long-range temporal correlations indicate that events in the past affect the development of the process in the future [13]. Therefore the relation between the hypnotazability level and the value of the EEG signals fractal dimension (Fig. 1) suggests that changing the level of the hypnosis susceptibility can affect the process of the past events and planning for future in the brain.

7. Conclusion

In the current study, it is tried to suggest a non-subjective pattern recognition system which can estimate the subject's hypnotizability level by measuring the EEG features. As the result of this study two features, based on the Higuchi's dimension of the signal's IMFs and the linear combination of the scaling exponent in theta band in channel C4, Petrosian's dimension and the Higuchi's dimension of the signal's IMFs in channel T6, were presented as the best features for classification of the three hypnosis susceptible groups. It was shown that based on the obtained results, a practical system could be designed that would be useful to clinicians to classify the subject's hypnotic susceptibility level instead of using traditional subjective methods which have different drawbacks. The results were also investigated in order to understand the neurophysiological aspect of brain mechanism under hypnosis. For continuing this research in order to complete the suggested system and designing a commercial type, the authors have different suggestions that put under consideration for their future works:

1- This investigation was performed on men. It is also suggested that additional examination be done on women, to demonstrate if sexuality can affect the obtained result or not.
2- In order to show the effect of the nature of the suggestions that have been used to induce hypnosis, it is proposed that the investigation is repeated on the subjects that were hypnotized by another induction method instead of Waterloo–Stanford group method.
3- Recently a new method was introduced to search for EEG characteristics during different mental tasks (i.e. learning in different ages [46], resting [47], Alzheimer [48] and Schizophrenia [49]) which analyzes multichannel EEG data as sequences of maps of the momentary spatial distributions of electric potential on the head surface. It became evident that brain activity over time consists of brief temporal epochs defined by a quasi-stable spatial distribution ('potential landscape') of brain electric activity; these epochs were called 'microstates,' and different microstates were found to incorporate different brain functions. In this study a method was suggested that can estimate hypnosis susceptibility level just after hypnosis induction based in the EEG dynamics, but it would be useful to estimate the level of hypnotizability during hypnosis induction (not at the end) or in other words monitoring the hypnosis trance depth changes instantaneously. Properties of certain classes of microstates vary with state of consciousness [50], therefore the changes of the microstates classes during hypnosis induction may be considered in index of hypnosis trance depth changes during hypnosis induction. We are working on this new method as the following of our research.

Conflict of interest statement

Not declared.

References

[1] M.E. Faymonville, M. Boly, S. Laureys, Functional neuroanatomy of the hypnotic state, J. Physiol. 99 (2006) 463–469.
[2] T. Isotani, D. Lehmann, R.D. Pascual-Marqui, K. Kochi, J. Wackermann, N. Saito, T. Yagyu, T. Kinoshita, K. Sasada, EEG source localization and global dimensional complexity in high- and low- hypnotizable subjects: a pilot study, Neuropsychobiology 44 (2001) 192–198.
[3] K.S. Bowers, Waterloo–Stanford group scale of hypnotic susceptibility, form C: manual and response booklet, Int. J. Clin. Exp. Hypn. 46 (3) (1998) 250–268.
[4] E. Cardea, D.B. Terhune, A note of caution on the waterloo-Stanford group scale of hypnotic susceptibility: a brief communication, Int. J. Clin. Exp. Hypn. 57 (2) (2009) 222–226.
[5] M. Heap, et al., The Highly Hypnotizable Person: Theoretical, Experimental, and Clinical Issues, Psychology Press, 2004.
[6] E.R. Hilgard, A Stage of Hypnosis: Two Decades of the Stanford Laboratory Hypnosis Research 1957–1979, Department of Psychology Stanford University, 1979.
[7] H.I. Kaplan, B.J. Sadock, Comprehensive Textbook of Psychiatry, Lippincott Willaims, 2000 chapter 30, 3: Hypnosis.
[8] I. Kirsch, et al., Experimental scoring for the waterloo-Stanford group scale, Int. J. Clin. Exp. Hypn. 46 (3) (1998) 269–279.
[9] R. Temes, Medical hypnosis: An introduction and Clinical Guide, Churchill Livingstone, 1999.
[10] D. Lehmann, P. Faber, T. Isotani, P. Wohlgemuth, Source locations of EEG frequency bands during hypnotic arm levitation: a pilot study, Contemp. Hypn. 18 (3) (2001) 120–127.
[11] G. Baghdadi, A.M. Nasrabadi, An investigation of changes in brain wave energy during hypnosis with respect to normal EEG, Sleep Hypn. 11 (2) (2009) 41–45.
[12] L. Stevens, et al., Binaural beat induced Theta EEG activity and hypnotic susceptibility: Contradictory results and technical considerations, Am. J. Clin. Hypn. 45 (4) (2003) 295–309.
[13] J.S. Lee, et al., Fractal analysis of EEG in hypnosis and its relationship with hypnotizability, Int. J. Clin. Exp. Hypn. 55 (1) (2007) 14–31.
[14] G. Baghdadi, A.M. Nasrabadi, Effect of hypnosis and hypnotizability on temporal correlations of EEG signals in different frequency bands, Eur. J. Clin. Hypn. 9 (1) (2009) 67–74.
[15] G. Baghdadi, A.M. Nasrabadi, Classifying hypnotizable groups, using EEG weighted regional frequency, Sci. Iran. 17 (1) (2010) 71–80.
[16] S..Cui, X. Li, G. Ouyang and X. Guan. Detection of epileptic spikes with empirical mode decomposition and nonlinear energy operator, in: International Symposium on Neural Networks, 2005.
[17] Y. Yu, C. Junsheng, A roller bearing fault diagnosis method based on EMD energy entropy and ANN, J. Sound Vib. 294 (2006) 269–277.
[18] A.M. Nasrabadi, Quantitative and qualitative evaluation of consciousness variation and depth of hypnosis through intelligent processing of EEG signals. Bioelectric Ph.D. Thesis, biomedical engineering department, Amirkabir university of Iran, 2002.
[19] J Emerson Raja, C.K. Loo, M.V.C. Rao, The necessity of a nonlinear and non-stationary data processing in engineering and the new Hilbert Huang Transform (HHT), College Science in India 1 (2007).
[20] D. Kim, H.S. Oh., EMD: A package for empirical mode decomposition and hilbert spectrum, R J. 1 (1) (2009) 40–46.
[21] M. Feldman, Theoretical analysis and comparison of the Hilbert transform decomposition methods, Mech. Syst. Signal Process. 22 (3) (2008) 509–519.
[22] M. Huang, P. Wu, Y. Liu, L. Bi and H. Chen. Application and contrast in brain–computer interface between Hilbert–Huang transform and wavelet transform, in: Proceedings of the Nineth International Conference for Young Computer Scientists, ICYCS 2008.

[23] N.E. Huang, et al., The empirical mode decomposition and the Hilbert spectrum for nonlinear and non-stationary time series analysis, Proc. R. Soc. London A 454 (1998) 903–995.
[24] H. Sharabaty, J. Martin, B. Jammes and D. Esteve Alpha and Theta wave localisation using Hilbert–Huang transform: empirical study of the accuracy. Information and Communication Technologies, ICTTA'06, 2006, Vol. 2, pp. 1159–1164.
[25] R. Panuszka, Z. Damijan, C. Kasprzak, Fractal EEG analysis with Higuchi's algorithm of low-frequency noise exposition on humans, J. Acoust. Soc. Am. 115 (5) . 2388–2388.
[26] R. Esteller, G. Vachtsevanos, J. Echauz, and B. Litt, A comparison of fractal dimension algorithms using synthetic and experimental data, in: Proceedings of IEEE International Symposium on Circuits and System, Adaptive Digital Signal Processing, 1999, Orlando, Fl, Vol. III, pp. 199–202.
[27] T. Costa, E. Rognoni, D. Galati, EEG phase synchronization during emotional response to positive and negative film stimuli, Neurosci. Lett. 406 (2006) 159–164.
[28] B. Scheltera and M. Winterhalder, Testing statistical significance of multivariate time series analysis techniques for epileptic seizure prediction, Chaos. 16:3108_1-3108_10 (2006).
[29] L. Sun, et al. Instantaneous frequency estimate of nonstationary phonocardiograph signals using Hilbert spectrum, in: Proceedings of the 2005 IEEE Engineering in Medicine and Biology, 2005, pp. 7285–7288.
[30] C.M..Sweeney-Reed, S.J. Nasuto, J.D..Howroyd and A.O. Andrade. Empirical mode decomposition for isolation of neural assemblies underlying cognitive acts, in: Proceedings of the Fourth IEEE EMBSS UK and Republic of Ireland Postgraduate Conference in Biomedical Engineering and Medical Physics, 2005, pp. 21–22.
[31] R.V. Hogg, J. Ledolter, Engineering Statistics, MacMillan Publishing Company, 1987.
[32] W.J. Krzanowski, Principles of Multivariate Analysis, Oxford University Press, 1988.
[33] G.J. McLachlan, Discriminant Analysis and Statistical Pattern Recognition, Wiley Interscience, 2004.
[34] W.J. Conover, Practical Nonparametric Statistics, Wiley, New York, 1980.
[35] J.N. Kok et al. IKNN: Informative K-nearest neighbor pattern classification, in: PKDD 2007, Proceedings of the Eleventh European Conference on Principles and Practice of Knowledge Discovery in Databases, 2007, LNAI 4702, pp. 248–264.
[36] B.V. Dasarathy, Nearest neighbor (NN) norms: NN pattern classification techniques, IEEE Computer Society Press, Los Alamitos, 1990.
[37] J. Ross, M.A. Persinger, Positive correlations between temporal lobe signs and hypnosis induction profiles: a replication, Percept. Mot. Skills 64 (1987) 828–830.
[38] Temporal Lobe, Langbrain. Rice University. 〈http://www.ruf.rice.edu/~lngbrain/cglidden/temporal.html〉. Retrieved 2 January (2011).
[39] J.F. Kihlstrom, F.J. Evans, E.C. Orne, M.T. Orne, Attempting to breach posthypnotic amnesia, J. Abnorm. Psychol. 89 (1980) 603–616.
[40] Al.A. Fingelkurts, An A. Fingelkurts, S. Kallio, A. Revonsuo, Cortex Functional Connectivity as a Neurophysiological correlates of hypnosis: an EEG case study, Neuropsychologia 45 (7) (2007) 1452–1462.
[41] S. Deivanayagi, M. Manivannan, P. Fernandez, Spectral analysis of EEG signals during hypnosis, Int. J. Syst. Cybernet. Inform. (2007) 75–80.
[42] N.F. Graffin, W.J. Ray, R. Lundy, EEG concomitants of hypnosis and hypnotic susceptibility, J. Abnorm. Psychol. 104 (1) (1995) 123–131.
[43] M.E. Sabourin, S.D. Cutcomb, H.J. Crawford, K. Pribram, EEG correlates of hypnotic susceptibility and hypnotic trance: Spectral analysis and coherence, Int. J. Psychophysiol. 10 (1990) 125–142.
[44] E. Kirmizialsan, Z. Bayraktaroglu, H. Gurvit, Y. Keskin, M. Emre, T. Demiralp, Comparative analysis of event-related potentials during Go/NoGo and CPT: Decomposition of electrophysiological markers of response inhibition and sustained attention, Brain Res. 1104 (1) (2006) 114–128.
[45] S. Kallio, A. Revonsuo, H. Hämäläinen, J. Markel, J. Gruzelier, Anterior brain functions and hypnosis:a test of the frontal hypothesis, Int. J. Clin. Exp. Hypn. 49 (2) (2001) 95–108.
[46] T. Koeniga, L. Prichep, D. Lehmannd, P.V. Sosa, E. Braeker, H. Kleinlogel, R. Isenhart, E.R. John, Millisecond by millisecond, year by year: normative EEG microstates and developmental stages, NeuroImage 16 (1) (2002) 41–48.
[47] D. Lehmann, H. Ozaki, I. Pal, E.E.G. Alpha Map, Series: brain micro-states by space-oriented adaptive segmentation, Electroen. Clin. Neuro. 1987 (67) (1987) 271–288.
[48] W.K. Strik, R. Chiaramonti, G.C. Muscas, M. Paganini, T.J. Mueller, A.J. Fallgatter, A. Versari, R. Zappoli, Decreased EEG microstate duration and anteriorisation of the brain electrical fields in mild and moderate dementia of the Alzheimer type, Psychiat. Res.: Neuroim. 75 (3) (1997) 183–191.
[49] S. Irisawa, et al., Increased omega complexity and decreased microstate duration in nonmedicated schizophrenic patients, Neuropsychobiology 54 (2) (2006) 134–139.
[50] D. Lehmann, R.D. Pascual-Marqui, C. Michel, EEG microstates, Scholarpedia 4 (3) (2009).